

AD-A194 968

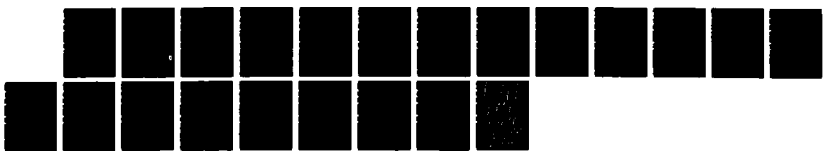
TUNABLE UV LASER PHOTOLYSIS OF NF₂: QUANTUM YIELD FOR
NF(A₁ DELTA) PRODUC (U) AEROSPACE CORP EL SEGUNDO CA
AEROPHYSICS LAB R F HEIDNER ET AL. 25 MAY 88
TR-8886A(2938-84)-1 SD-TR-88-38

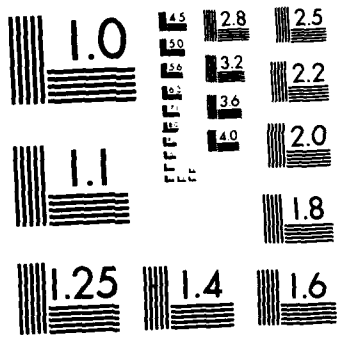
1/1

UNCLASSIFIED

F/G 9/3

NL





AD-A194 960

Tunable UV Laser Photolysis of NF_2 : Quantum Yield for $NF(a^1\Delta)$ Production

R. F. HEIDNER, H. HELVAJIAN,
and J. B. KOFFEND
Aerophysics Laboratory
Laboratory Operations
The Aerospace Corporation
El Segundo, CA 90245

25 May 1988

Prepared for
SPACE DIVISION
AIR FORCE SYSTEMS COMMAND
Los Angeles Air Force Base
P.O. Box 92960, Worldway Postal Center
Los Angeles, CA 90009-2960

DTIC
SELECTED
JUN 17 1988
S E D

APPROVED FOR PUBLIC RELEASE:
DISTRIBUTION UNLIMITED

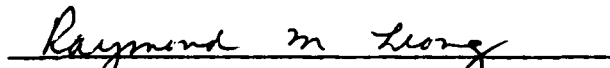
This report was submitted by The Aerospace Corporation, El Segundo, CA 90245, under Contract No. F04701-85-C-0086-P00016 with the Space Division, P.O. Box 92960, Worldway Postal Center, Los Angeles, CA 90009-2960. It was reviewed and approved for The Aerospace Corporation by W. P. Thompson, Director, Aerophysics Laboratory. Lt Scott W. Levinson, SD/CNW, was the project officer for the Mission-Oriented Investigation and Experimentation (MOIE) program.

This report has been reviewed by the Public Affairs Office (PAS) and is releasable to the National Technical Information Service (NTIS). At NTIS, it will be available to the general public, including foreign nationals.

This technical report has been reviewed and is approved for publication. Publication of this report does not constitute Air Force approval of the report's findings or conclusions. It is published only for the exchange and stimulation of ideas.



SCOTT W. LEVINSON, Lt, USAF
MOIE Project Officer
SD/CNW



RAYMOND M. LEONG, Maj, USAF
Deputy Director, AFSTC West Coast Office
AFSTC/WCO OL-AB

REPORT DOCUMENTATION PAGE

1a. REPORT SECURITY CLASSIFICATION Unclassified			1b. RESTRICTIVE MARKINGS			
2a. SECURITY CLASSIFICATION AUTHORITY			3. DISTRIBUTION / AVAILABILITY OF REPORT Approved for public release; distribution unlimited.			
2b. DECLASSIFICATION / DOWNGRADING SCHEDULE						
4. PERFORMING ORGANIZATION REPORT NUMBER(S) TR-0086A(2930-04)-1			5. MONITORING ORGANIZATION REPORT NUMBER(S) SD-TR-88-38			
6a. NAME OF PERFORMING ORGANIZATION The Aerospace Corporation Laboratory Operations		6b. OFFICE SYMBOL (if applicable)	7a. NAME OF MONITORING ORGANIZATION Space Division			
6c. ADDRESS (City, State, and ZIP Code) El Segundo, CA 90245			7b. ADDRESS (City, State, and ZIP Code) Los Angeles Air Force Base Los Angeles, CA 90009-2960			
8a. NAME OF FUNDING / SPONSORING ORGANIZATION		8b. OFFICE SYMBOL (if applicable)	9. PROCUREMENT INSTRUMENT IDENTIFICATION NUMBER F04701-85-C-0086-P00016			
8c. ADDRESS (City, State, and ZIP Code)			10. SOURCE OF FUNDING NUMBERS			
			PROGRAM ELEMENT NO.	PROJECT NO.	TASK NO.	WORK UNIT ACCESSION NO.
11. TITLE (Include Security Classification) Tunable UV Laser Photolysis of NF_2 : Quantum Yield for $\text{NF}(a^1\Delta)$ Production						
12. PERSONAL AUTHOR(S) Heidner, Raymond F., III; Helvaian, Henry; and Koffend, J. Brooke						
13a. TYPE OF REPORT		13b. TIME COVERED FROM _____ TO _____		14. DATE OF REPORT (Year, Month, Day) 1988 May 25		15. PAGE COUNT 18
16. SUPPLEMENTARY NOTATION						
17. COSATI CODES			18. SUBJECT TERMS (Continue on reverse if necessary and identify by block number)			
FIELD	GROUP	SUB-GROUP				
			NF_2 Photodissociation, Photolysis, Quantum yield, <i>Nitrogen difluoride</i>			
19. ABSTRACT (Continue on reverse if necessary and identify by block number)						
<p>The ultraviolet photodissociation of difluoroamine (NF_2) has been investigated from 240 to 270 nm, using tunable UV radiation from a frequency-upconverted YAG pumped dye laser system. The absorption cross section of NF_2 and the photolysis quantum yield for the fragment $\text{NF}(a^1\Delta)$ were measured with 0.25 cm⁻¹ resolution. The $\text{NF}(a^1\Delta)$ quantum yield decreases at longer wavelengths and is only 1% at 260 nm. This suggests that the first long wavelength band in NF_2 leads primarily to ground state $\text{NF}(X^3\Sigma)$, and that the existence of a new higher lying NF_2 electronic state is responsible for the $\text{NF}(a^1\Delta)$ production.</p> <p style="text-align: right;"><i>Keynote</i></p>						
20. DISTRIBUTION / AVAILABILITY OF ABSTRACT <input checked="" type="checkbox"/> UNCLASSIFIED/UNLIMITED <input type="checkbox"/> SAME AS RPT <input type="checkbox"/> DTIC USERS			21. ABSTRACT SECURITY CLASSIFICATION Unclassified			
22a. NAME OF RESPONSIBLE INDIVIDUAL			22b. TELEPHONE (Include Area Code)		22c. OFFICE SYMBOL	

CONTENTS

I.	INTRODUCTION.....	5
II.	EXPERIMENTAL.....	7
III.	RESULTS AND DISCUSSION.....	13
	A. NF_2 Absorption Spectrum.....	13
	B. $\text{NF}(a^1\Delta)$ Quantum Yield.....	15
	C. $\text{NF}(a^1\Delta)$ Appearance Lifetime.....	17
IV.	CONCLUSIONS.....	19
	REFERENCES.....	21

FIGURES

1a. Schematic diagram of the experimental apparatus used to measure NF_2 absorption spectrum..... 8

1b. The experimental apparatus used to measure the $\text{NF}(a^1\Delta)$ quantum yield..... 9

2. The NF_2 absorption spectrum..... 14

3. The absolute $\text{NF}(a^1\Delta)$ quantum yield from UV photolysis of NF_2 16

Accession For	
NTIS GRA&I	<input checked="" type="checkbox"/>
DTIC TAB	<input type="checkbox"/>
Unannounced	<input type="checkbox"/>
Justification	
By	
Distribution/	
Availability Codes	
Dist	Avail and/or Special
A-1	



1. INTRODUCTION

In 1985, Colburn and Kennedy were successful in synthesizing tetrafluorohydrazine, N_2F_4 , a reagent that has sufficient reactivity to be of chemical interest¹ yet is stable enough to be manipulated. Initial room temperature experiments with mixtures of low molecular weight alkanes and N_2F_4 showed no chemical change. By increasing the temperature and/or irradiating the mixtures with a mercury resonance lamp, a reaction could be initiated. Colburn, Johnson and coworkers were able to verify that the parent compound N_2F_4 thermally dissociates into difluoroamine, NF_2 , radicals.² Both the observed UV band absorption at 260 nm and the increase in reactivity were attributed to the NF_2 radical.^{3,4} Since those initial experiments, the chemistry of NF_2 with various hydrocarbons has been studied. It has also been shown that the addition-elimination reaction between H and NF_2 radicals produces $NF(a^1\Delta)$ with very high quantum efficiency (>90%).⁵⁻⁷ The $NF(a^1\Delta)$ product is both radiatively and collisionally metastable, making it a convenient energy storage molecule. In the past few years, there has been further interest in understanding the chemistry of NF_2/N_2F_4 by those who anticipate its use in semiconductor processing.

We report the results of an experiment designed to study the tunable ultraviolet (UV) photolysis of NF_2 and to measure the photolysis quantum yield of $NF(a^1\Delta)$ radicals. Tunable photolysis of small molecules in conjunction with state-resolved product distributions can yield information concerning the fundamental dynamics of the photofragmentation process and the electronic structure of the parent.⁸⁻¹⁶ For example, from a study of the I^* quantum yield, Hofmann and Leone¹⁰ showed that the long-wavelength part of the HgI_2 UV absorption consists of two distinct components. A similar investigation¹⁵ of the photolysis of ICN revealed that its first absorption continuum comprises three separate bands.

In the case of NF_2 , Collins and Husain¹⁷ carried out an experiment in which NF_2 photolysis was studied in the vacuum UV (126-140 nm). A series of diffuse bands was attributed to Rydberg transitions of NF_2 . Other transient

II. EXPERIMENTAL

Tunable UV radiation was generated using a Qantel Datachrome 581C Nd-YAG pumped dye laser system by frequency-doubling the output from the dye laser and subsequently mixing it with the 1060 nm fundamental wavelength. KDP crystals cut at different angles were used for both frequency-doubling and mixing. Several red dye mixtures (DCM, LDS698, and LDS700) were used to obtain UV light over the range studied. The bandwidth (FWHM) of the red dye laser wavelength, measured with a solid etalon, was 0.10 cm^{-1} . Combining this spectral bandwidth with the width of the 1060 nm mixing radiation, our UV resolution was 0.25 cm^{-1} . A small 4 nm gap near 257 nm resulted from the dye combinations we selected. The energies in the nominally 5 nsec laser pulses ranged from 0.3 to 3 mJ, depending upon the wavelength.

The experimental apparatus for measuring the NF_2 absorption cross section and $\text{NF}(a^1\Delta)$ quantum yields were arranged with slight modifications, as represented in Fig. 1. The NF_2 handling system was common to both arrangements: Mixtures of N_2F_4 (Hercules, 96%) and Ar (Matheson, 99.995%) were stored at 90 psia in a 4 liter stainless steel cylinder. The $\text{N}_2\text{F}_4/\text{Ar}$ mixture was admitted into one end of the cylindrical photolysis cell and flowed slowly past the observation region. The cells, which are Pyrex with quartz windows at each end, were enclosed in an oven that was maintained at 185°C . A thermocouple gauge measured the oven temperature near the observation region. Under these conditions, the N_2F_4 is 99% dissociated into NF_2 radicals.¹⁸⁻³⁰ The gas pressure was measured near the observation region with a capacitance manometer. The total pressures ranged from 1 to 8 Torr, which resulted in NF_2 partial pressures from 0.10 to 0.80 Torr.

The NF_2 absorption spectra were produced using the apparatus depicted in Fig. 1a. Because the doubled dye laser beam and the infrared (IR) laser can most efficiently be mixed at a specified phase-matching angle, the sum UV radiation appears at a slight angle to the collinear fundamental and doubled dye laser beams. Using two uncoated quartz beamsplitters, the summed UV radiation could be spatially selected and directed through the 37-cm-long

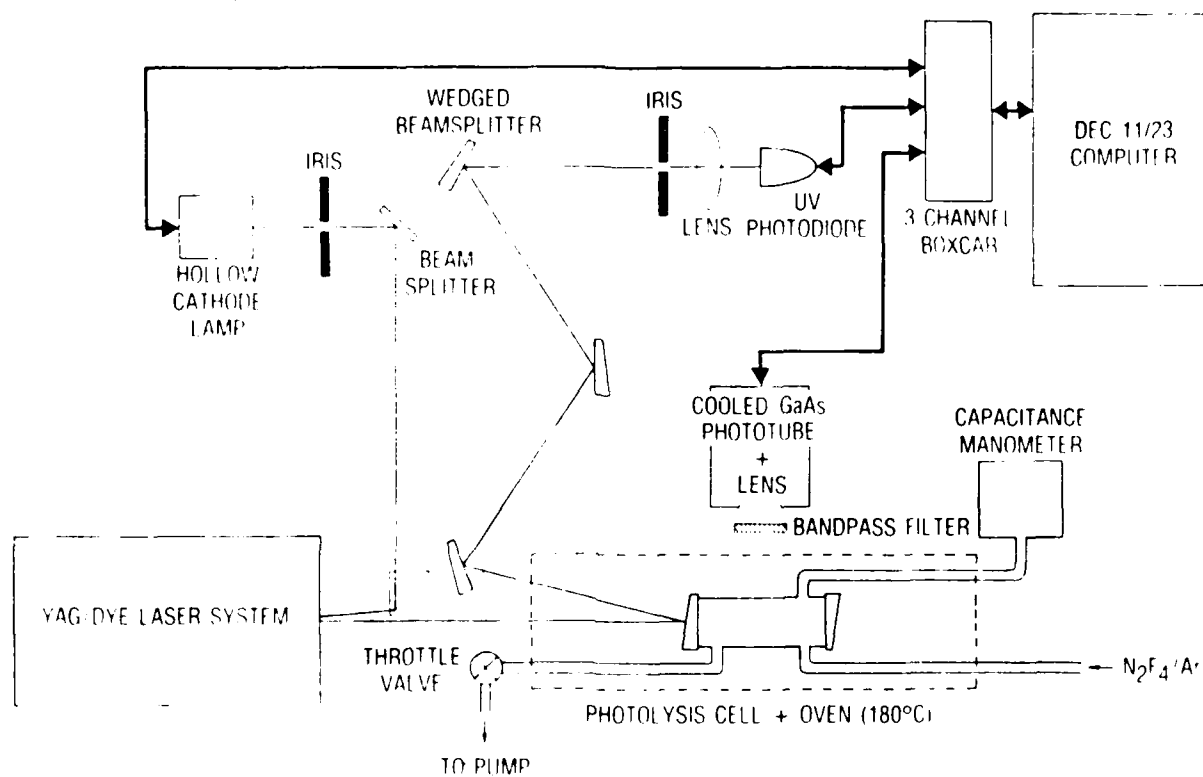


Fig. 1b. The experimental apparatus used to measure the $\text{NF}(a^1\Delta)$ quantum yield. The shorter photolysis cell facilitates the calculation of laser photolysis flux at the observation region.

absorption cell. A bandpass interference filter was also placed in the path to prevent any scattered fundamental and doubled dye laser light from reaching the detectors. To ensure minimal NF_2 dissociation, the laser energy was attenuated ($\geq 10^7$) by first passing it through the bandpass filter and then through numerous beamsplitters. The beamsplitters, as well as the cell windows, are uncoated quartz Suprasil flats that are wedged to avoid interference effects as the laser is tuned. A total of three additional beamsplitters were placed before and after the cell to reduce the flux incident upon the two matched silicon photodiodes. The dual-beam arrangement was tested for linearity by constructing several stacks of quartz windows (test "absorbers") whose transmittances were previously measured at several fixed wavelengths using a Beckman UV 5240 spectrophotometer. Transmission through the cell for the range of NF_2 densities used was typically between 45% and 90%. During a laser scan, the fundamental and doubled beams were reflected into a hollow cathode lamp operating with neon. The lamp provided absolute wavelength calibration from the opto-galvanic effect whenever the laser was resonant with neon or neon ion transitions. A three-channel boxcar integrator processed the signals from the lamp and the two photodiodes. As the laser was scanned, the output from each channel was digitized and stored by a DEC 11/23 computer for subsequent analysis. The laser repetition rate was 10 Hz; the dye laser was scanned at 0.02 nm sec^{-1} .

The arrangement used in the $\text{NF}(a^1\Delta)$ quantum yield study is displayed in Fig. 1b. The absorption cell was replaced by a shorter, 10-cm-long, photolysis cell, and the laser was not attenuated. A narrow bandpass filter (0.4 nm FWHM), centered at the $\text{NF } a - X (0,0)$ band²⁴ at 874 nm, was placed in front of a cooled GaAs photomultiplier in order to monitor the fluorescence from the $\text{NF}(a^1\Delta)$ photofragment. Under our experimental conditions, the maximum NF_2 photolysis fraction did not exceed 3%. The laser power was monitored by directing the reflection from the front surface of the cell's entrance window to a photodiode. Several wedged beamsplitters were positioned to sufficiently attenuate the reflected laser beam before it hit the diode. As explained in the absorption studies above, a hollow cathode lamp was used for absolute wavelength calibration. Again, the three-channel boxcar in conjunction with the DEC computer recorded the quantum yield spectra.

We also performed time-resolved studies of the $\text{NF}(a^1\Delta)$ fluorescence following UV photolysis. In these experiments, the signal from the phototube was recorded with a Transiac model 2001 transient digitizer (100 MHz) and was averaged by the DEC computer.

III. RESULTS AND DISCUSSION

A. NF₂ ABSORPTION SPECTRUM

The NF₂ absorption spectrum, presented in Fig. 2, was generated from the ratio of the signal and reference photodiode signals (Fig. 1a). Figure 2 was constructed from several overlapping laser scans and represents an average of several different NF₂ partial pressures within each scan. We estimate an error of 5% for the absorption cross sections in Fig. 2. We recorded the cell transmission both at 248 nm and at the peak of the band absorption, 260 nm, for ten different NF₂ pressures between 0.2 and 0.8 Torr. The absorbance plotted versus [NF₂] was linear and passed through the origin. The absorption cross section at the KrF wavelength (248.5 nm) is $6.74(0.34) \times 10^{-19} \text{ cm}^2$.

As previously shown by Goodfriend and Woods,¹⁹ the 260 nm band of NF₂ (3 cm⁻¹ spectral resolution) is observed to be a continuum overlaid with diffuse structure. It is clearly evident from Fig. 2 that, with our higher resolution of 0.25 cm⁻¹, the NF₂ spectrum exhibits no additional structure. Indeed, the diffuse structure in the spectrum of Ref. 19 is more prominent when compared with our data. The experiment in Ref. 19 was performed at room temperature, whereas ours was performed at 185°C. This spectral difference is probably due to the inherently different ground state NF₂ rovibrational distributions between the two experiments. The spectra of Kuznetsova et al.,²⁰ obtained at temperatures between 150 and 200°C, resemble more closely those in our work. It should be noted that absorption by N₂F₄ does not occur in the 260 nm region and only becomes important for wavelengths below 210 nm.

The NF₂ absorption cross section at 248.5 nm reported above is in excellent agreement with that of Ref. 21, $6.1(0.6) \times 10^{-19} \text{ cm}^2$. However, at 260 nm, there is considerable discrepancy among the values measured at room temperature. They vary from³¹ $5.2 \times 10^{-19} \text{ cm}^2$ to as high as^{18,27} $1.8 \times 10^{-18} \text{ cm}^2$. Although our work was performed at 185°C, our results ($1.5 \pm 0.1 \times 10^{-18} \text{ cm}^2$) appear to support the higher values. This is particularly striking since the NF₂ peak cross section shows a negative temperature dependence,¹⁸ and therefore we would expect our measured value to be lower. As was mentioned by

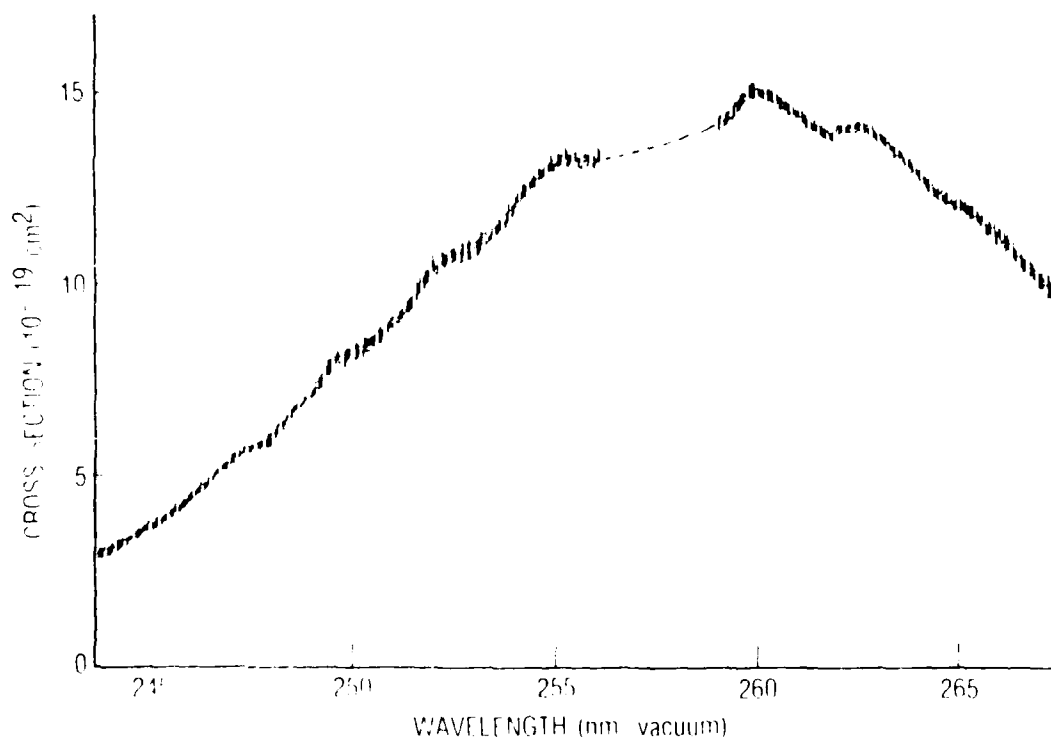


Fig. 2. The NF_2 absorption spectrum. The region in dashed lines signifies the wavelengths that could not be produced by the photolysis laser.

Evans and Tschuikow-Roux,¹⁸ the disagreement among the earlier studies³¹⁻³⁴ may be reconciled by attributing it to experimental conditions for which the Beer-Lambert law is not valid.

B. NF(a¹Δ) QUANTUM YIELD

The NF(a¹Δ) quantum yield from the photolysis of NF₂ is plotted as a function of wavelength in Fig. 3. As with the NF₂ absorption spectrum (Fig. 2), this curve is constructed from several overlapping scans, and, again, several NF₂ densities were used for each scan. The relative NF(a¹Δ) quantum yield was calculated using the following expression:

$$\phi_{\text{NF}(a^1\Delta)} = \frac{\text{SNF}(a^1\Delta)}{I(L) \sigma(\lambda)} \quad (1)$$

where SNF(a¹Δ) is the NF(a¹Δ) signal, I(L) is the relative photolysis intensity at the observation point L, and σ(λ) is the NF₂ absorption cross section. The quantum efficiency of the photodiode varies only by 0.4% over the wavelength region covered and was neglected. We converted the relative quantum yield determined in this work to an absolute measurement, using the results of Ref. 21, in which a value of 0.10±0.05 was reported for KrF excimer laser photolysis.

We observe that the NF(a¹Δ) quantum yield decreases at longer wavelengths. At the peak of the NF₂ absorption near 260 nm, the quantum yield is only 1%, indicating that upper state in this transition leads primarily to ground state NF. Goodfriend and Woods¹⁹ assign the 260 nm band of NF₂ to the transition ²A₁ - ²B₁. The next excited state is also predicted to have ²A₁ symmetry. A qualitative examination of the electronic symmetry correlation between NF₂ states and possible dissociation products reveals that the first ²A₁ state can lead to NF(X³Σ) as well as to NF(a¹Δ). A correlation to NF(b¹Δ) is also present, but formation of this NF electronic state is endothermic for the photolysis wavelengths in this work. However, dissociation from the next ²A₁ NF₂ electronic state can also form NF(a¹Δ) and NF(b¹Δ) species but must

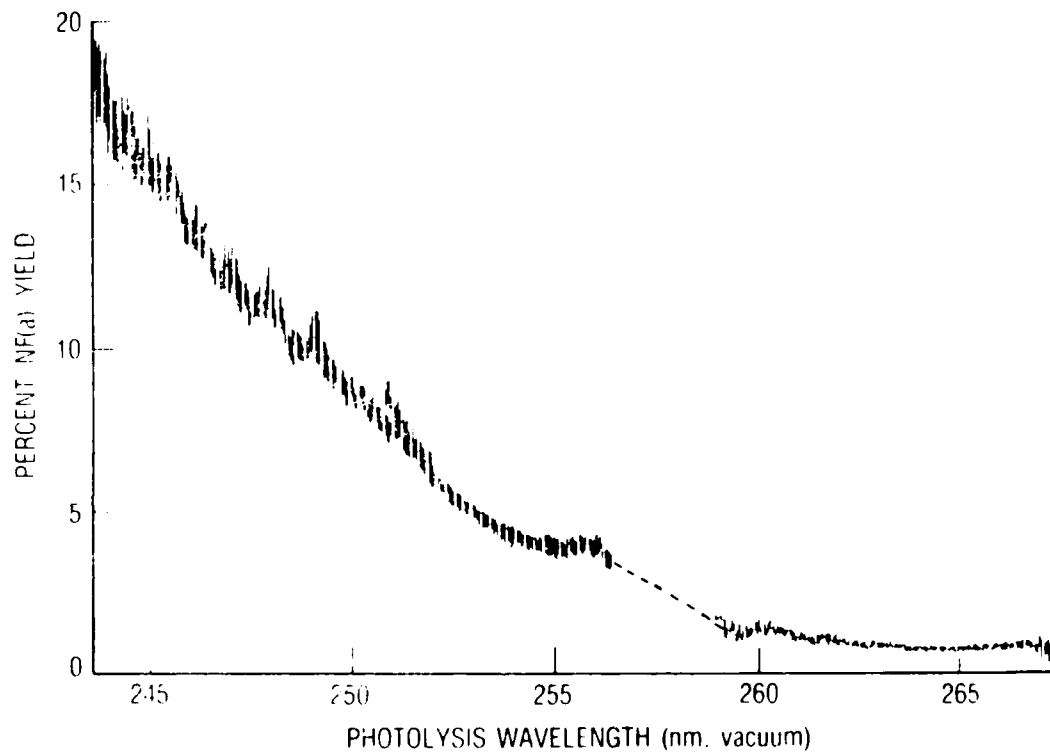


Fig. 3. The absolute $\text{NF}(a^1\Delta)$ quantum yield from UV photolysis of NF_2 .

curve-cross to form the $NF(X^3\Sigma)$ product. Our results support the existence of a new, higher lying NF_2 electronic state that leads to $NF(a^1\Delta)$ formation. Under our experimental conditions, it was difficult for us to use wavelengths shorter than 240 nm and still maintain an adequate signal-to-noise ratio. From Fig. 2, the absorption cross section as measured at 243.6 nm is $2.2 \times 10^{-19} \text{ cm}^2$, which is sufficiently small that the signal-to-noise ratio for $NF(a^1\Delta)$ emission at 243.6 nm photolysis decreases by a factor of 4 relative to photolysis at 260 nm (see Fig. 3). Kuznetsova et al.²⁰ were able to measure the absorption further to the UV than we were, and they have identified a band at 237.7 nm. A careful study of the spectra presented in Ref. 20 reveals an absorption slightly larger than that predicted by a Gaussian decay, suggesting a weakly allowed second transition. Using this observation and our results for the existence of a "new" higher lying NF_2 electronic state, we can say that the quantum yield in this region is significantly larger than at 260 nm, although the absorption cross section is small.

C. $NF(a^1\Delta)$ APPEARANCE LIFETIME

An extremely intriguing result is our observation that the production of $NF(a^1\Delta)$ from the photolysis of NF_2 does not occur promptly after the 15 nsec KrF laser pulse but is delayed by 80 μsec . This result contrasts with the diffuse structure observed in the absorption spectrum, which is perhaps more indicative of a predissociation. In previous work²¹ done in this laboratory, evidence was presented that this effect is not due to an impurity or from secondary reactions of the photolysis products. In this work, we observed similar results at several different photolysis wavelengths (248.5, 251, and 260 nm). The $NF(a^1\Delta)$ risetimes were independent of NF_2 density ($0.87\text{--}3.1 \times 10^{16} \text{ molec cm}^{-3}$), buffer gas pressure (1-6 Torr Ar), and photolysis wavelength (243-260 nm). These results could reflect a mechanism whereby $NF_2(A)$ undergoes an intersystem crossing to another electronic state prior to dissociation. In the case of isoelectronic ClO_2 , absorption bands below 400 nm ($A^2A_2 - X^2B_1$) exhibit line broadening and the predominant dissociation mechanism has been attributed to spin orbit coupling of the 2A_2 with nearby 2A_1 and/or 2B_1 vibronic states.³⁵⁻³⁶ In NF_2 , the lowest excited states have 2A_1 , 2A_1 , 2B_2 , and 2A_2 electronic symmetry.¹⁹ The NF_2 2A_1 electronic states

could be perturbed by the excited 2B_2 electronic states. Antisymmetric vibrations $\nu_3(b_1)$ excited in the 2A_1 electronic state could lead to a 2B_1 vibronic symmetry, such as the ground state. These arguments are supported by the diffuse absorption spectrum, which we measure in the 260 nm band for NF_2 . We believe that following laser excitation of NF_2 , the excited NF_2^* species are temporarily "trapped" in an intermediate state from which dissociation to $NF(a^1\Delta) + F$ occurs. If the specific NF_2^* dissociating state were to be in equilibrium with another NF_2^* state (perhaps the "trapped" state) and the rate for dissociation were much faster (at the buffer densities used in the experiment) than the rate of approach to equilibrium, then the rate of $NF(a^1\Delta)$ production will show no pressure dependence. A more careful experiment in which the time-resolved NF_2 photolysis is conducted in a low pressure cell or in the free jet expansion of a molecular beam may be necessary. We are currently pursuing experiments to monitor the appearance of $NF(X^3\Sigma)$ using the laser-induced fluorescence technique, and also to monitor possible emission from electronically excited NF_2^* .

IV. CONCLUSIONS

We have studied the UV photodissociation of NF_2 from 240 to 270 nm. The absorption cross section of NF_2 was measured, and the photolysis quantum yield for the $\text{NF}(a^1\Delta)$ fragment was determined. We observe that the first long-wavelength absorption band in NF_2 leads primarily to ground state $\text{NF}(X^3\Sigma)$. Our results also support the existence of a new, higher lying NF_2 electronic state that is responsible for $\text{NF}(a^1\Delta)$ production. From the spectra of Kuznetsova et al.²⁰ and our results, we postulate that the transition to this new state is much weaker than that leading to the 260 nm band absorption. Using the assignments of Goodfriend and Woods,¹⁹ it is possible that this new state is also 2A_1 . We have observed that the anomalously long $\text{NF}(a^1\Delta)$ appearance lifetime is independent of NF_2 density, buffer gas pressure, and photolysis wavelength. We had previously²¹ shown that this appearance time could not be due to impurities. This long $\text{NF}(a^1\Delta)$ appearance time, along with the structureless absorption spectrum, allows us to postulate that the photolysis of NF_2 to form $\text{NF}(a^1\Delta)$ is indirect, possibly occurring via an intersystem crossing to another electronic state.

REFERENCES

1. C. B. Colburn and A. Kennedy, J. Amer. Chem. Soc. **80**, 5004 (1958).
2. F. A. Johnson and C. B. Colburn, J. Amer. Chem. Soc. **83**, 3034 (1961).
3. L. H. Piette, F. A. Johnson, K. A. Booman, and C. B. Colburn, J. Chem. Phys. **35**, 1481 (1961).
4. C. B. Colburn and F. A. Johnson, J. Chem. Phys. **33**, 1869 (1960).
5. J. M. Herbelin and N. Cohen, Chem. Phys. Lett. **20**, 603 (1973).
6. J. M. Herbelin, Chem. Phys. Lett. **42**, 367 (1976).
7. R. J. Malins and D. W. Setser, J. Chem. Phys. **85**, 1342 (1981).
8. R. D. Clear, S. J. Riley, and K. R. Wilson, J. Chem. Phys. **63**, 1340 (1975).
9. A. B. Petersen and I. W. M. Smith, Chem. Phys. **30**, 407 (1978).
10. H. Hofmann and S. R. Leone, J. Chem. Phys. **69**, 3819 (1978).
11. M. S. de Vries, N. J. A. van Veen, and A. E. de Vries, Chem. Phys. Lett. **56**, 395 (1978).
12. T. G. Lindeman and J. R. Wiesenfeld, J. Chem. Phys. **70**, 2882 (1979).
13. L. C. Lee and D. L. Judge, J. Chem. Phys. **63**, 2782 (1975).
14. M. Kawasaki, S. J. Lee, and R. Bersohn, J. Chem. Phys. **71**, 1235 (1979).
15. W. M. Pitts and A. P. Baronavski, Chem. Phys. Lett. **71**, 395 (1980).
16. J. B. Koffend and S. R. Leone, Chem. Phys. Lett. **81**, 136 (1981).
17. R. J. Collins and D. Husain, J. Photochem. **2**, 459 (1972).
18. P. J. Evans and E. Tschuikow-Roux, J. Chem. Phys. **10**, 4202 (1976).
19. P. L. Goodfriend and H. P. Woods, J. Mol. Spectrosc. **13**, 63 (1964).
20. L. A. Kuznetsova, Yu. Ya. Kuzyakov, and T. M. Tatevskii, Opt. Spectrosc. **16**, 295 (1964).
21. J. B. Koffend, C. E. Gardner, and R. F. Heidner III, J. Chem. Phys. **83**, 2904 (1985).

22. J. T. Herron and V. H. Diebler, J. Chem. Phys. 33, 1595 (1960).
23. A. E. Douglas and W. E. Jones, Can. J. Phys. 44, 2251 (1966).
24. W. E. Jones, Can. J. Phys. 45, 21 (1967).
25. B. de B. Darwent, Natl. Bur. Stand. Ref. Data Ser. 31 (1970).
26. C. T. Chean and M. A. A. Clyne, J. Photochem. 15, 21 (1981).
27. F. A. Johnson and C. B. Colburn, J. Am. Chem. Soc. 83, 3043 (1961).
28. S. N. Foner and R. L. Hudson, J. Chem. Phys. 58, 581 (1973).
29. A. P. Modica and D. F. Hornig, J. Chem. Phys. 49, 629 (1968).
30. P. J. Evans and E. Tschuikow-Roux, J. Phys. Chem. 82, 182 (1978).
31. M. A. A. Clyne and J. Connor, J. Chem. Soc. Faraday Trans. 2. 68, 1220 (1972).
32. L. M. Brown and B. de B. Darwent, J. Chem. Phys. 42, 2158 (1965).
33. K. O. MacFadden and E. Tschuikow-Roux, J. Phys. Chem. 77, 1475 (1973).
34. G. L. Schott, L. S. Blair, and J. D. Morgan, Jr., J. Phys. Chem. 77, 2823 (1973).
35. P. A. McDonald and K. K. Innes, Chem. Phys. Lett. 59, 562 (1978).
36. H. Hamada, A. J. Merer, S. Michielsen, and S. Rice, J. Mol. Spectrosc. 86, 499 (1981).

LABORATORY OPERATIONS

The Aerospace Corporation functions as an "architect-engineer" for national security projects, specializing in advanced military space systems. Providing research support, the corporation's Laboratory Operations conducts experimental and theoretical investigations that focus on the application of scientific and technical advances to such systems. Vital to the success of these investigations is the technical staff's wide-ranging expertise and its ability to stay current with new developments. This expertise is enhanced by a research program aimed at dealing with the many problems associated with rapidly evolving space systems. Contributing their capabilities to the research effort are these individual laboratories:

Aerophysics Laboratory: Launch vehicle and reentry fluid mechanics, heat transfer and flight dynamics; chemical and electric propulsion, propellant chemistry, chemical dynamics, environmental chemistry, trace detection; spacecraft structural mechanics, contamination, thermal and structural control; high temperature thermomechanics, gas kinetics and radiation; cw and pulsed chemical and excimer laser development including chemical kinetics, spectroscopy, optical resonators, beam control, atmospheric propagation, laser effects and countermeasures.

Chemistry and Physics Laboratory: Atmospheric chemical reactions, atmospheric optics, light scattering, state-specific chemical reactions and radiative signatures of missile plumes, sensor out-of-field-of-view rejection, applied laser spectroscopy, laser chemistry, laser optoelectronics, solar cell physics, battery electrochemistry, space vacuum and radiation effects on materials, lubrication and surface phenomena, thermionic emission, photo-sensitive materials and detectors, atomic frequency standards, and environmental chemistry.

Computer Science Laboratory: Program verification, program translation, performance-sensitive system design, distributed architectures for spaceborne computers, fault-tolerant computer systems, artificial intelligence, micro-electronics applications, communication protocols, and computer security.

Electronics Research Laboratory: Microelectronics, solid-state device physics, compound semiconductors, radiation hardening; electro-optics, quantum electronics, solid-state lasers, optical propagation and communications; microwave semiconductor devices, microwave/millimeter wave measurements, diagnostics and radiometry, microwave/millimeter wave thermionic devices; atomic time and frequency standards; antennas, rf systems, electromagnetic propagation phenomena, space communication systems.

Materials Sciences Laboratory: Development of new materials: metals, alloys, ceramics, polymers and their composites, and new forms of carbon; non-destructive evaluation, component failure analysis and reliability; fracture mechanics and stress corrosion; analysis and evaluation of materials at cryogenic and elevated temperatures as well as in space and enemy-induced environments.

Space Sciences Laboratory: Magnetospheric, auroral and cosmic ray physics, wave-particle interactions, magnetospheric plasma waves; atmospheric and ionospheric physics, density and composition of the upper atmosphere, remote sensing using atmospheric radiation; solar physics, infrared astronomy, infrared signature analysis; effects of solar activity, magnetic storms and nuclear explosions on the earth's atmosphere, ionosphere and magnetosphere; effects of electromagnetic and particulate radiations on space systems; space instrumentation.

ENID

DATED

FILM

8-88
DTIC